Figure 1 shows an Arrhenius plot of the temperature dependence of the mechanical damping of $RBa_2Cu_3O_{7-\delta}$ in equilibrium with an ambient atmosphere of 20% O_2 in N_2 for R = Y, Gd, Nd, and La. As anticipated, the relaxation peaks at a fixed frequency of 40 kHz were displaced to progressively lower temperatures (543°, 408°, 374°, and 350°C, respectively) as the rare-earth size was increased. Over this temperature range, the relaxation for $YBa_2Cu_3O_{7-\delta}$ is thermally activated with a single activation energy of motion $h_m \sim 1.04$ eV (*5*). At the location of the mechanical damping maxima, the enhancements in mobility over that for R = Y are, respectively, 19, 48, and 97 times for R = Gd, Nd, and La. These major enhancements occur in the temperature range that is relevant for loading oxygen. The temperatures T_m for maximum damping and the enhancements in diffusion coefficients are also listed in Table 1.

Oxygen self-diffusion coefficients, D, may be estimated by assuming that the damping, Q^{-1}, is governed by a single Debye relaxation, which is thermally activated. Thus

$$Q^{-1} = Q_0^{-1}\omega\tau/(1+\omega^2\tau^2) \quad (1)$$

where ω is the frequency and τ is the relaxation time, and

$$\tau = \tau_0 exp(h_m/kT) \quad (2)$$

where k is the Boltzmann constant. Oxygen diffusion occurs by two-dimensional hopping between the O1 and O5 sites, so that

$$D = f\ell^2/4\tau \quad (3)$$

where f is the correlation factor and $\ell \sim 2.76$ Å is the hop distance between the O1 and O5 sites. The temperature dependence of D or τ is large compared with that of f, so we assume for convenience $f \sim 1$. The values of D thus calculated (plotted in Fig. 2) show a clear progression to higher oxygen diffusion rates in lattices containing the larger rare-earth ions. At a fixed temperature of 400°C the enhancements in D over that for Y-123 are 19, 30, and 56 times for Gd-, Nd-, and La-123, respectively. The diffusion coefficient relevant to oxygen loading is the chemical diffusion coefficient, which is related to the self-diffusion coefficient, measured here, by a factor that describes the dependence of the oxygen stoichiometry, δ, on oxygen partial pressure. Kishio *et al.* (*12*) reported the temperature and oxygen partial pressure dependence of δ at equilibrium to be very similar for Y-123 and Nd-123. We therefore expect that the large enhancements in diffusion coefficient reported here will also be reflected in oxygen chemical diffusion coefficients.

Data from the tails of the relaxation peaks are not reliable because of the dominance there of background damping and because of the large excursion from tuned resonance, which we imposed in mid-temperature range by trimming the length of both the sample and the quartz spacer rod. The Nd-123 data appear to be particularly affected in this way. The data are also critically dependent on the quality of the ceramic joint between the sample and the spacer rods. We have extended measurements to much longer relaxation times (~24 hours) by examining the transient relaxation of structure at room temperature by in situ x-ray diffraction after quenching from elevated temperatures into liquid N_2. The same trend in enhanced mobility with the larger rare earths is preserved, but the enhancements are much smaller (approximately fourfold) (*13*).

REFERENCES AND NOTES

1. S. M. Fortier and B. J. Giletti, *Science* **245**, 1481 (1989).
2. C. G. Vayenas, S. Bebelis, S. Ladas, *Nature* **343**, 625 (1990).
3. B. C. H. Steele, *Electronic Ceramics* (Elsevier, New York, 1991).
4. J. D. Jorgensen *et al.*, *Phys. Rev. B* **41**, 1863 (1990).
5. J. L. Tallon and M. P. Staines, *J. Appl. Phys.* **68**, 3998 (1990).
6. J. L. Tallon *et al.*, *Physica C* **171**, 61 (1990).
7. A. Manthiram, S. J. Lee, J. B. Goodenough, *J. Solid State Chem.* **73**, 278 (1988).
8. R. G. Buckley *et al.*, *Physica C* **174**, 383 (1991).
9. J. L. Tallon *et al.*, *ibid.* **185–189**, 855 (1991).
10. J. L. Tallon, A. H. Schuitema, N. E. Tapp, *Appl. Phys. Lett.* **52**, 507 (1988).
11. S. J. Rothman, J. L. Routbort, U. Welp, J. E. Baker, *Phys. Rev. B* **44**, 2326 (1991).
12. K. Kishio *et al.*, *Mater. Res. Soc. Symp. Proc.* **156**, 91 (1989).
13. J. L. Tallon and B.-E. Mellander, in preparation.
14. R. D. Shannon, *Acta Crystallogr. Sect. A* **32**, 751 (1976).

15. We are grateful to the New Zealand Foundation for Science, Research, and Technology and to the Electricity Corporation of New Zealand for funding this research. We thank R. G. Buckley and W. H. Robinson for discussing aspects of this work.

29 May 1992; accepted 25 August 1992

Nanochannel Array Glass

R. J. Tonucci, B. L. Justus, A. J. Campillo, C. E. Ford

The fabrication and characterization of a glass containing a regular parallel array of submicrometer channels or capillaries are described. The capillaries are arranged in a two-dimensional hexagonal close packing configuration with channel diameters as small as 33 nanometers and packing densities as high as 3×10^{10} channels per square centimeter. The high-temperature stability of the nanochannel glass array is well suited as a host or template for the formation of quantum confined semiconductor structures or as a mask for massively parallel patterned lithographic applications.

Quantum confined systems imbedded in a protective or interactive matrix have generated considerable interest in both basic research and commercial applications because of their unique electronic and optical properties and their possible use as components in ultrasmall and ultradense electronic devices (*1*, *2*). One such approach to fabricating quantum confined structures has been to utilize a host or template structure. Very small chambers or voids within the host can be filled with material in which the walls of the void confine the volume of material being deposited. If the voids are sufficiently small (*3*), quantum confinement may occur in the material and its associated quantized effects observed by a variety of optical and electronic measurements. Examples utilizing this technique to create quantum confined systems with II-VI and III-V semiconductor materials have been demonstrated in a variety of host structures such as zeolites (*4*), plastics (*5*, *6*), sol-gels (*7*, *8*), and Vycor glass (*9*, *10*).

Nanochannel glass (NCG) hosts and masks with uniformly shaped voids in large arrays exhibit a high packing density of parallel voids or channels with channel diameters as small as a few tens of nanometers (*11*). There are greater than 10^6 channels in a typical array and excellent control is maintained over the geometric regularity in the placement of channel positions as well as the depth of channel formation.

The fabrication of this NCG material is inspired by a draw process not unlike the way optic fibers and microchannel plates are made (*12*, *13*). Recent attempts at drawing single glass fibers have succeeded in producing hollow (*14*) and metal-filled (*15*) cores as small as a few tenths of a micrometer. The smallest previously reported high-density glass fiber arrays made by a drawing process containing greater than 10^6 channels exhibited channel diameters of approximately 2 μm (*16*).

Nanochannel glass arrays are prepared by arranging dissimilar glasses, of which at

R. J. Tonucci, B. L. Justus, A. J. Campillo, Optical Sciences Division, Naval Research Laboratory, Washington, DC 20375.
C. E. Ford, Ni-Tec Division, Varo Inc., Garland, TX 75041.

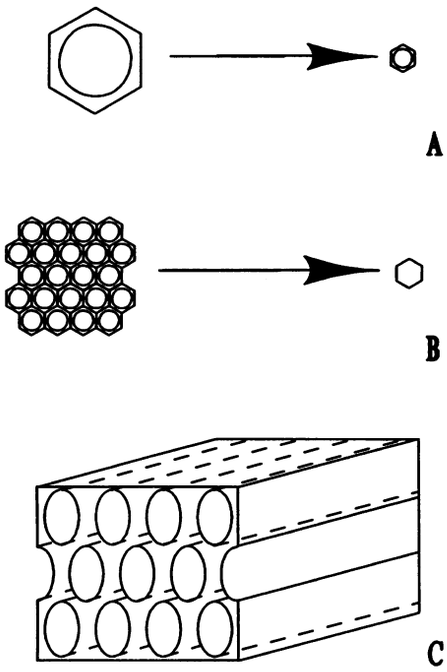

Fig. 1. Schematic diagram indicating the steps for fabricating the NCG array. (**A**) Cladding and acid-etchable core glass are reduced in diameter to a fine filament by drawing the glass composite at elevated temperatures. (**B**) After stacking the filaments into a bundle forming an array, the bundle is further drawn to reduce its overall diameter again to a filament. The process is repeated until the desired diameter of the channel glass is achieved. (**C**) A magnified view of the final product of an array of acid-etchable cores embedded in the matrix glass.

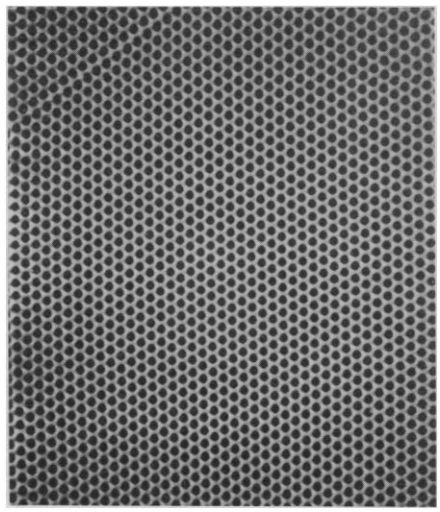

Fig. 2. A SEM micrograph of 450-nm-diameter hollow channels arranged in a hexagonal close packing array configuration contained within the matrix glass. A 10-nm film of gold was deposited on the surface of the array to prevent charging during SEM analysis. The section shown is 26 μm in width.

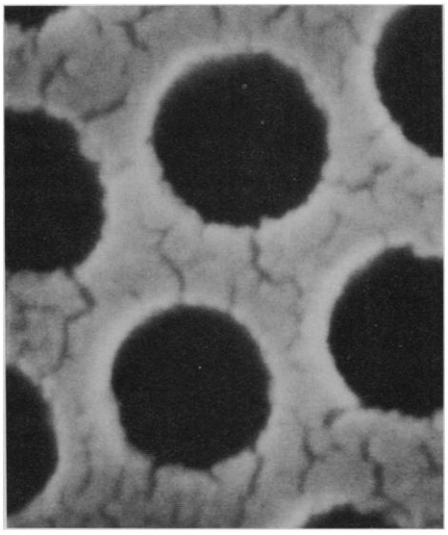

Fig. 3. A high-resolution SEM micrograph of a 95-nm-diameter channel array indicating the regularity of the geometric pattern and roundness of the channel diameters. The section shown is 296 nm in width.

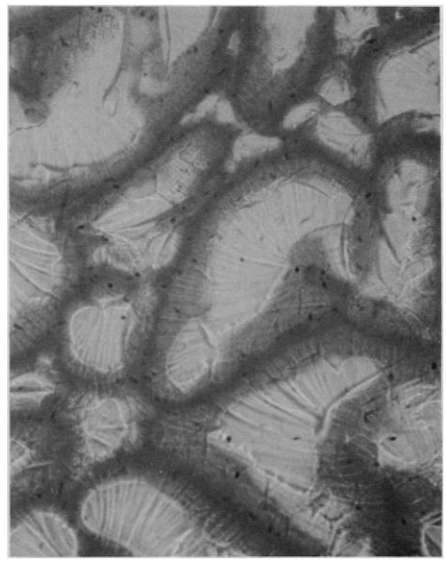

Fig. 4. An optical micrograph of an unannealed NCG sample indicating regions of high stress between the intersection of the etched and unetched portions of the channel interface. Sections where the glass fractured below the etched portion of the array appear as lightly colored regions. The dark regions indicate the etched portion of the glass. The section shown is 445 μm in width.

least one glass type is usually acid etchable, in a predetermined configuration. Construction of the array starts by insertion of a cylindrical acid-etchable glass rod (which will also be referred to as the channel glass) into an inert glass tube (which will also be referred to as the matrix glass) whose inner dimensions match that of the rod (Fig. 1A). The pair is then drawn at high temperature under vacuum to reduce the overall cross section to that of a fine filament. The filaments are then stacked in a bundle, refused, and redrawn (Fig. 1B). This process is continued until appropriate channel diameters and the desired number of array elements are achieved. Careful consideration must be given to drawing conditions and the materials used. Interdiffusion of the two glass materials at elevated temperatures will cause a reduction in the definition of a channel after etching. In an extreme case, the sample becomes a homogeneous glass after repeated exposures to elevated temperatures. Annealing of the glass composite is necessary if the glass materials chosen are susceptible to work hardening. By adjusting the ratio of the diameter of the etchable glass rod to that of the outside dimension of the inert glass tubing, we can cause the center-to-center spacing of the rods and their diameters in the finished product to become independently adjustable parameters. A view of the finished product is shown in Fig. 1C.

For the NCG array hosts described in this report, a clear potash lead glass (*17*) was chosen as a suitable matrix glass. It has good working characteristics at elevated temperatures and a relatively low optical absorption coefficient in the visible portion of the spectrum. The low optical absorption coefficient is an important consideration for optical characterization of quantum confined materials deposited into the channels, as well as for its potential use in electro-optic device applications. The channel glass chosen is a boron-rich acid-etchable glass whose composition is compatible with the matrix glass in its working characteristics. Although a variety of suitable channel glass materials are available, glass types were sought with etch rates of at least several thousand times that of the matrix glass to prevent distortion of the array channels during the etching process. An inert glass cladding, similar in composition to the matrix material, was added to the circumference of the NCG array structure during the final draw for protection of the array edge during the various processing stages and later as a support structure for characterization.

Once the fabrication process is complete, the NCG material is cut perpendicular to the direction of the channels with a diamond saw to produce 0.5- to 5-mm sections of material. The ends of the sections are ground with diamond compound and final polished to an optical flat with 0.5-μm diamond powder. The channel glass of the array structure is then etched with a hydrochloric acid solution in water, after a thorough cleaning with methanol to remove any surface contamination. Immediately following the etching process, the samples are rinsed three times in distilled

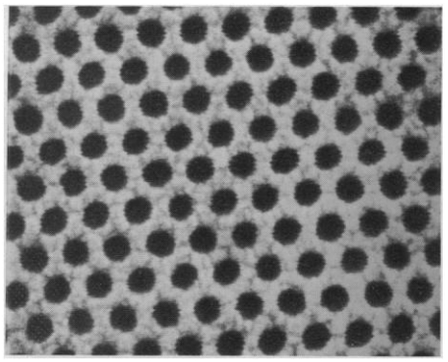

Fig. 5. A high-resolution SEM micrograph of a 33-nm-diameter channel array. The horizontal lines in the figure are a result of SEM rastering at high magnification. The astigmatism of the SEM at this resolution can be seen to distort the regularity of some of the channel diameters. The section shown is 600 nm in width.

water, followed by a methanol rinse and then dried. Careful control over the duration of the total etch time was maintained for each sample.

Spatial measurements on the geometry and regularity of channel diameters in the array were made with a Hitachi model S-800 field ion scanning electron microscope (SEM). An 8- to 9-nm layer of gold was evaporated onto the NCG to prevent charging during SEM operation. Samples were mounted vertically on the SEM specimen holder for channel diameter and geometric measurements. Figure 2 shows a SEM micrograph of a hexagonal close packing (HCP) arrangement of channel glasses in relief, after acid etching. The sample contains approximately 5×10^6 channels and is uniform throughout. The channel diameter is approximately 450 nm, and the center-to-center spacing is approximately 750 nm. Figure 3 shows a similar high-resolution SEM micrograph with 90-nm channel diameters. The geometry of the circular channel circumference in this sample is seen to be well preserved at these small channel diameters. The rough edges of the channels and apparent cracking of the surface are primarily the result of incomplete layering of a thin gold film deposited on the NCG surface and are not indicative of the NCG array itself.

When the glass structures were prepared as described above, it was found that most samples exhibited varying degrees of fracturing and were very fragile. Gentle tapping of the sample caused the etched portion of the rod to crumble and separate from the unetched portion and cladding, especially after deep etching. Examination of the boundary of the etched-unetched interface showed a conchoidal fracture consistent with a strained interface (Fig. 4). In this figure, the dark regions are what remains of the bottom of the etched channels and the light regions indicate sections of unetched glass. It was found that when the same samples are fine annealed, and then repolished and etched as before, the samples become very durable. Stress within the etched and remaining composite glass material is relieved considerably by the annealing process and from such results it is possible to make ultrathin sections of NCG material.

Ultimately, use of the NCG material for basic research in nanometer science and technology requires very small channels and precise control over semiconductor placement. In applications requiring strong confinement of semiconductor materials or in the fabrication of quantum devices incorporating quantum tunneling effects, constraints on channel uniformity and location become much more stringent, especially if cooperative interactions are a consideration. The NCG material has been fabricated in large arrays with channels a few tens of nanometers in diameter. Figure 5 shows an array of 33-nm-diameter channels with approximately 20 nm of spacing between channel edges at their closest point. Channel diameters are extremely regular throughout the entire extent of the array and the array is extremely uniform in its geometric regularity. The jagged edges along the channel circumference are due to SEM rastering at high magnification. Astigmatism in the SEM also contributes to some of the channels appearing to have an irregular shape.

The ability of the NCG material to withstand temperatures in excess of 600°C without deformation makes this material well suited for a variety of semiconductor and metal-deposition processes. Semiconductor systems such as the III-V and II-VI groups can be deposited into the NCG by metal organic chemical vapor deposition (MOCVD) requiring temperatures just over 400°C to drive reactions to completion (*18*). Depending upon the etch depth of the channels, arrays of ultrasmall semiconductor wires and dots can be fabricated with highly uniform dimensions.

Laterally patterned array architectures in quantum well–type structures can be made by ion implantation through the channels of an NCG mask. The thickness of the mask must usually be kept greater than a few micrometers or a gold coating must be used to keep accelerated energetic ions from passing through the solid glass portions of the NCG. It is possible to remove much of the damage caused to the quantum well portion of the sample and return the system to a relaxed lattice-matched condition by standard annealing techniques. Masks have been fabricated to study the effects of nanometer-scale direct writing of both positive and negative images on energy sensitive surfaces. The NCG material has considerable potential for a variety of other applications including lensing and collimating of neutral beams such as x-rays (*19*) and neutrons (*20, 21*), high-temperature nanometer ultrasharp cutoff filters for solid, liquid, and gas systems, and ultradense electronic and memory device fabrication applications, to name a few.

REFERENCES AND NOTES

1. See for instance, the special section in *Science* [**254**, 1300 (1991)] and references therein.
2. A good overview of current research efforts in the field of nanostructures can be found in W. P. Kirk and M. A. Reed [*Nanostructures and Mesoscopic Systems* (Academic Press, New York, 1992)].
3. Dimensions of interest in semiconductors are on the order of the effective size of an exciton, the lowest electronic excited state in a semiconductor, whose energy is derived from an interaction between the localization and mutual attraction between an electron and a hole that comprise the exciton. The radius of an exciton can vary from a few angstroms to hundreds of nanometers depending upon the material.
4. G. D. Stucky and J. E. Mac Dougall, *Science* **247**, 669 (1990).
5. Y. Wang and W. Mahler, *Optics Commun.* **61**, 233 (1987).
6. J. P. Kuczynski, B. H. Milosavljevic, J. K. Thomas, *J. Phys. Chem.* **88**, 980 (1984).
7. T. Rajh, M. I. Vucemilovic, N. M. Dimitrjevic, O. I. Micic, A. J. Nosik, *Chem. Phys. Lett.* **143**, 305 (1988).
8. H. Minti, M. Eyal, R. Reisfield, G. Berkovic, *ibid.* **183**, 201 (1991).
9. J. C. Luong, *Superlattices Microstruct.* **4**, 385 (1988).
10. Y. Wang and N. Herron, *Res. Chem. Intermed.* **15**, 17 (1991).
11. R. J. Tonucci, B. L. Justus, A. J. Campillo, in *International Conference on Quantum Electronics Technical Digest Series 1992* (Optical Society of America, Vienna, 1992), vol. 9, p. 60.
12. D. Washington, V. Duchenois, R. Polaert, R. M. Beasley, *Acta Electron.* **14**, 201 (1971).
13. J. L. Wisa, *Nucl. Instrum. Methods Phys. Res. A* **162**, 587 (1979).
14. P. Engstrom *et al.*, *ibid.* **302**, 547 (1991).
15. E. F. Skelton *et al.*, *Science* **253**, 1123 (1991).
16. B. N. Laprade and S. T. Reinhart, *Soc. Photo. Instrum. Eng.* **1072**, 119 (1989); B. N. Laprade and M. Corbett, *Low Noise, Ultra Small Pore Curved Channel Microchannel Plate Development Program* (Galileo Electro-Optics Corp., Sturbridge, MA, 1988).
17. Corning glass type 8161, Corning Glass Works, Corning, NY 14831.
18. T. F. Kuech, *Mat. Sci. Rep.* **2**, 1 (1987); Y. Wang and N. Herron, *Res. Chem. Interm.* **15**, 17 (1991).
19. K. A. Nugent, H. N. Chapman, S. W. Wilkins, A. W. Stevenson, T. J. Davis, *Soc. Photo. Instrum. Eng.* **1319**, 516 (1990).
20. M. A. Kumakhov and V. A. Sharov, *Nature* **357**, 390 (1992).
21. H. Chen *et al.*, *ibid.*, p. 391.

22. One of the authors (R.J.T.) would like to acknowledge the help of J. Ruller at the Naval Research Laboratory for her help in annealing glass samples. This work was supported by the Office of Naval Research and the Defense Advanced Research Projects Agency ULTRA program.

21 August 1992; accepted 2 October 1992